VOL. 24, NO. 2, 2025, 98-103
elektrika.utm.my
ISSN 0128-4428

ELEKTRIKA
Journal of Electrical Engineering

A Comparative Study of Four Defected Ground Structures for Ultra-wideband Planar Antenna Application at 3.5 GHz

Nisaa Yasmin bt Nor Izuddin[1*], **Osman bin Ayop**[1] and **Farid bin Zubir**[1]

[1]Faculty of Electrical Engineering, Universiti Teknologi Malaysia, 81310 UTM Skudai, Johor, Malaysia.

[*]Corresponding author: nisaayasmin@graduate.utm.my

Abstract: Advancements in wireless communication systems have spurred the development of enhanced antennas to meet diverse application requirements. Ultra-wideband (UWB) technology, recognized for its broad frequency range, is crucial for enabling various wireless services, particularly within the expanding 5G network. This study compares four different Defected Ground Structures (DGS) integrated with a UWB antenna to function as a band-stop filter at lower (< 3 GHz) and higher (> 5 GHz) frequency bands, while allowing the critical frequency around 3.5 GHz to operate. The UWB planar antenna, designed on an FR-4 substrate material with a half ground plane, incorporates four distinct slots as filters from 2.7 GHz to 2.8 GHz and 5.3 GHz to 10.5 GHz to mitigate interference. Each DGS configuration's performance was evaluated through simulation, assessing return loss, S-parameters, and radiation characteristics. Results showed that DGS Design 2 provided the best outcome, with a deep stopband centered at 3.5 GHz and minimal impact on efficiency, realized gain, and surface current. This study offers insights into optimizing DGS designs for UWB antenna applications. The antenna design and simulations were conducted using CST Microwave Studio software to enhance performance for advanced wireless communication systems.

Keywords: Ultra-wideband, defected ground structure, band-stop

Article History: received 10 March 2024; accepted 7 August 2024; published 31 August 2025

1. INTRODUCTION

The growing demand for high-speed wireless communication has driven communication systems to develop enhanced antennas capable of meeting diverse application needs [1]. Ultra-wideband (UWB) technology [2], renowned for its ability to transmit data over a broad frequency spectrum, has become pivotal in enabling various wireless communication services, particularly within the expanding realm of 5G networks [3]. To harness the full capabilities of UWB technology, antennas must not only cover a wide frequency range but also exhibit exceptional performance characteristics [4]. This research delves into the field of antenna engineering, with a focus on integrating Defected Ground Structure (DGS) into UWB antennas.

Wireless communication systems now require compact and high-performance radio frequency (RF) components [5]. To reduce noise and improve the power that an amplifier can generate, modern communication systems must suppress the harmonics due to the stringent spectrum laws that are in place globally [6].

The utilization of UWB technology in modern wireless communication systems has brought about unparalleled possibilities for rapid data transmission, short-range communication, and location-based applications [7]. Nevertheless, unlocking the complete capabilities of UWB faces hurdles due to inherent challenges in UWB antenna designs, including bandwidth constraints, less-than-ideal radiation efficiency, and vulnerability to interference [8].

The incorporation of DGS into UWB antennas has demonstrated potential in tackling these obstacles. DGS has been integrated into planar transmission lines like microstrip lines, coplanar waveguides [9], and conductor-backed coplanar waveguides on the ground plane [10]. Defects introduced on the ground plane disrupt the current distribution of the ground plane, altering the characteristics of the transmission line by introducing additional parameters such as slot resistance, slot capacitance, and slot inductance to the line parameters (line resistance, line capacitance, and line inductance) [11]. In other words, any defect in the ground plane modifies the effective capacitance beneath the microstrip line and the microstrip line inductance by incorporating slot resistance, inductance, and capacitance. DGS is straightforward to design and manufacture, and its corresponding circuit is easy to implement [12].

2. DESIGN AND ANALYSIS

There are three sections to this work. Firstly, a basic planar antenna is developed to get an UWB frequency with an operating frequency of 3.5 GHz for it to be able to operate in the 5G sub-6 GHz spectrum. Next is developing a few suitable designs for the DGS that can be used as a stopband to focus on the antenna's 3.5 GHz working frequency.

Lastly, the developed DGS is integrated with the UWB planar antenna.

2.1 Ultra-wideband Antenna

To design a UWB antenna, the process begins by determining an anticipated size derived from the center frequency of the UWB antenna. Utilizing FR4 as the material and employing microstrip antenna design principles, the initial dimensions for the UWB antenna are calculated using the microstrip antenna formula [13].
The patch dimension, L can be written as:

$$L = \frac{c}{2f\sqrt{\varepsilon_{eff}}} - 2\Delta l$$

$$\Delta L = 0.412h\frac{(\varepsilon_{reff} + 0.3)(\frac{W}{h} + 0.264)}{(\varepsilon_{reff} - 0.258)(\frac{W}{h} + 0.8)}$$

$$\varepsilon_{reff} = \left(\frac{\varepsilon_r + 1}{2}\right) + \left[\left(\frac{\varepsilon_r - 1}{2}\right)\left[1 + 12\frac{h}{W}\right]^{-0.5}\right]$$

Where:

f = Operating frequency
ε_r = Permittivity of the dielectric
ε_{reff} = Permittivity of the dielectric
W = Patch's width
L = Patch's length
h = Thickness of the dielectric

The W is not the critical value but can be selected as:

$$W = \frac{c}{2f}\sqrt{\frac{2}{\varepsilon_r + 1}}$$

Since the substrate is FR4, the specification of the substrate is, a dielectric constant ε_r =4.6 and a loss tangent of 0.019. The thickness of the substrate h =1.6 mm, for the antenna.

The antenna is constructed of three layers as shown in Figure 1: a ground plane is at the bottom, a substrate is situated in the center, and the patch is at the top. Initially designed as a simple rectangular patch, the patch's shape is modified to get an operating frequency of 3.5 GHz with a UWB range. Modifications of the rectangular patch are made into a 4-step staircase of different length that has a triangular extension, connecting the patch and transmission line for impedance matching. The modified patch is from copper with a thickness of h =0.035 mm.

The middle layer of the antenna is a substrate made of FR-4 with a relative permittivity of ε_r = 4.6 and a thickness of 1.6 mm. The substrate is 35 mm in length and 30 mm in width.

The last layer is a half-ground plane made of copper with a thickness of 0.035 mm and a size of 16 mm in length and 30 mm in width. The reference dimensions of the one layer of substrate antenna are labelled and given in Table 1. The dimension of the DGS is designed to resonate at 3.5GHz, which corresponds to the antenna's center frequency.

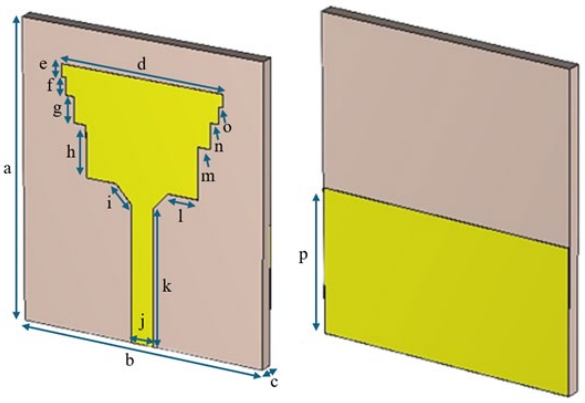

Figure 1. Illustration of front and back view of UWB antenna with one layer of substrate.

Table1. Dimensions of UWB antenna with one layer of substrate

Parameters	Dimension (mm)
a	35.00
b	30.00
c	1.60
d	20.00
e	1.50
f	2.00
g	3.00
h	6.00
i	2.73
j	2.79
k	16.00
l	3.75
m	1.50
n	1.00
o	0.50
p	16.00

2.2 Defected Ground Structure (DGS)

The stopband features of DGS are widely recognized particularly for their structural properties. There are four shapes of DGS designed and simulated, called DGS 1, 2, 3, and 4. Figure 2 shows four different configurations of DGS at the ground plane.

2.3 Development of DGS 1, 2, 3 and 4

2.3.1 DGS Design Evolution

The progression of the Defected Ground Structure (DGS) from version 1 to 4 has demonstrated refinements in design intricacy, optimizing its electromagnetic properties and enhancing its ability to act as a stopband filter, thereby providing improved electromagnetic interference mitigation and enhanced performance in diverse electronic

and communication systems. The early stages of the design were based on a V-shaped DGS [14], then the design improvement process was done by doing a parametric study on the shapes by identifying the related frequency on the surface current and using a transmission line method for the DGS designs as shown in Figure 3 to get the operating frequency of each DGS designs.

The illustration of unit cell for DGS 1, 2, 3 and 4 is shown in Figure 2. The structure is incorporated on the ground plane of the UWB antenna with 1 layer of substrate by defecting the ground plane with the DGS shape. The reference dimension of the DGS is labelled and shown in Table 2.

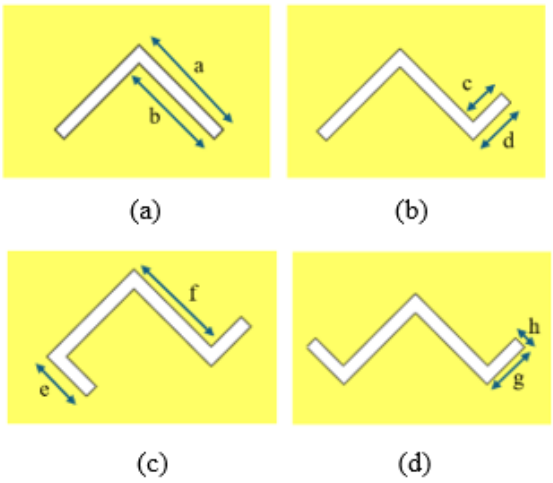

Figure 2. DGS Designs (a) DGS 1 (b) DGS 2 (c) DGS 3 (d) DGS 4

Table 2. Dimensions of DGS 1, 2, 3 and 4

Parameters	Dimension (mm)
a	4.38
b	3.88
c	1.51
d	2.00
e	2.00
f	3.88
g	2.00
h	0.50

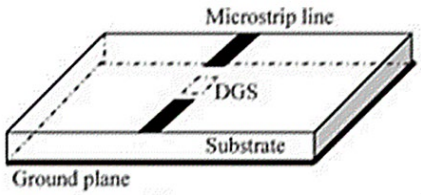

Figure 3. 3-D view of DGS with two weakly coupled microstrip line [15].

2.3.2 S21 Characterization of DGS 1, 2, 3 and 4

The S21 performance of DGS are shown in Figure 4. The characterization shows the resonant frequency that the DGS acts as a stopband for an UWB antenna with an operating frequency of 3.5 GHz.

Though useful, a DGS achieving only -10 dB suppression at the operating frequency indicates limitations. Unlike Electromagnetic Band Gap (EBG) structures that can achieve wider stopbands exceeding -20 dB due to their electromagnetic bandgap properties, DGS relies on resonances, making precise control and deep suppression challenging [16]. Additionally, DGS can suffer from leakage currents. While simpler to design and potentially more compact, EBG offers superior suppression due to their periodic nature and is preferred when a very deep stopband and precise frequency control are crucial.

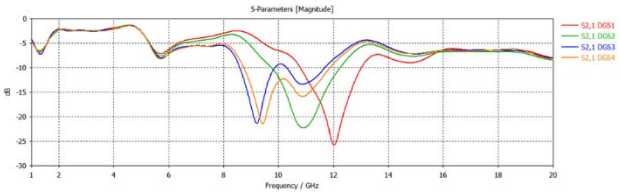

Figure 4. S21 of DGS 1, 2, 3 and 4.

The optimum antenna configuration is the fusion of the wideband antenna integrated with the DGS at the ground plane. The DGS functions as a stopband by selectively suppressing the frequencies at the S11 parameter. The sharpness of the filter is determined by the length of the DGS traversing across the transmission line [9].

2.4 Final Antenna Design

The final antenna design is the integration of DGS with the UWB antenna. The DGS is integrated into the back of the ground plane of the UWB antenna as shown in Figure 5.

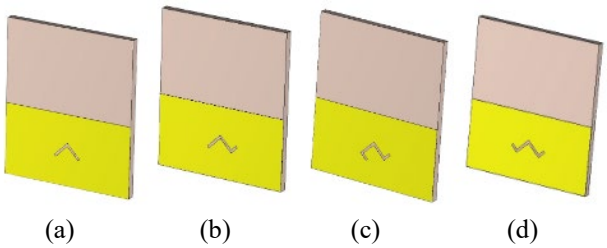

Figure 3. Back view of UWB planar antenna with (a) DGS 1 (b) DGS 2 (c) DGS 3 (D) DGS4.

The aim is to enhance antenna performance, particularly in terms of bandwidth, gain, and radiation pattern. The DGS, strategically placed beneath the antenna's radiating patch, acts as a band-stop filter, suppressing unwanted frequencies and reducing interference, thus improving the antenna's efficiency and signal quality [17]. By properly designing the DGS, it is possible to achieve frequency notch characteristics, which can help in mitigating interference from nearby frequency bands. Integrating the DGS with a UWB antenna allows for the exploitation of

its inherent benefits, such as high data rates, low power consumption, and resistance to multipath fading. The UWB antenna, designed to operate over a broad frequency range with minimal distortion, complements the DGS's frequency-selective characteristics [18], resulting in an overall optimized performance across the UWB spectrum.

3. SIMULATION RESULTS AND DISCUSSION

Figure 6. illustrates the simulated magnitude of the reflection coefficient, S11 for an UWB antenna without DGS and with DGS 1, DGS 2, DGS 3 and DGS 4. The magnitude of S11 is taken from below -10 dB for all simulated frequency for determining its operating frequency. From the simulated figure, it shows that the DGS managed to act as a stopband for unwanted frequencies.

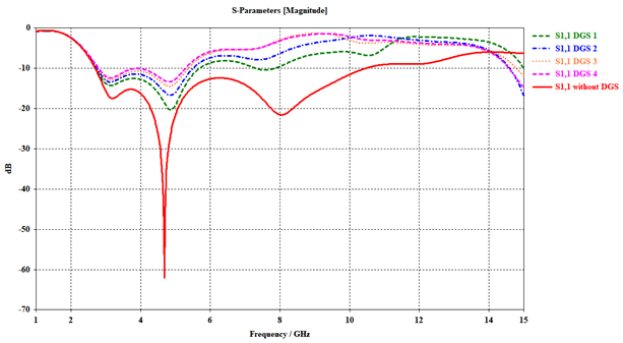

Figure 4. Simulation of S11 Parameters of UWB Antenna without DGS and with DGS 1, 2, 3 and 4

From the graph in Figure 7, it is evident that DGS 1 exhibits the highest total efficiency compared to DGS 2, 3, and 4 at 3.5 GHz. Additionally, the graph illustrates that frequencies within the stopband regions correspond to lower total efficiency values. This proves that the DGS manages to act as the stopband for unwanted frequencies from the UWB antenna. While highly beneficial, incorporating a DGS into an antenna can cause a slight dip in efficiency, typically up to 7% compared to the design without one. This efficiency loss stems from the DGS disrupting current flow in the ground plane, introducing resistance and potentially causing some current to leak through unintended paths.

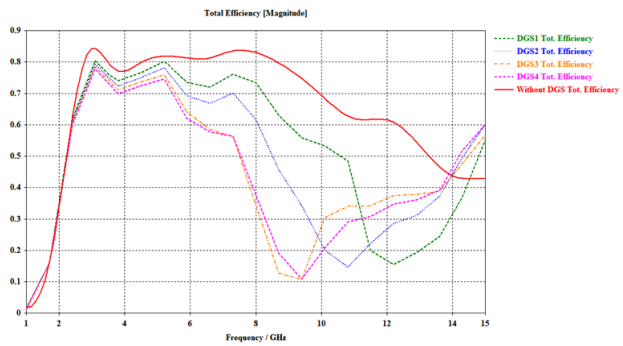

Figure 5. Total efficiency of UWB Antenna without DGS and with DGS 1, 2, 3 and 4

The realized gain of a UWB antenna experiences a significant contrast in stopband control and general effectiveness when comparing instances with and without DGS. Without DGS, the realized gain graph of the UWB antenna reveals fluctuations and inconsistencies within the stopband section, leading to undesired signal leakage and interference. However, the addition of DGS within the antenna's design effectively functions as stopbands by suppressing undesired radiation across specific frequency ranges.

This improvement is clearly depicted in the realized gain graph, where the presence of DGS results in enhanced stopband performance characterized by more distinct roll-offs and improved suppression of unwanted frequencies. The realized gain value in Figure 8 can decrease from 4 to -2.5 at stopband frequencies. As a result, integrating DGS structures not only boosts the overall realized gain of the UWB antenna but also ensures superior stopband management, ultimately contributing to heightened antenna performance in UWB applications.

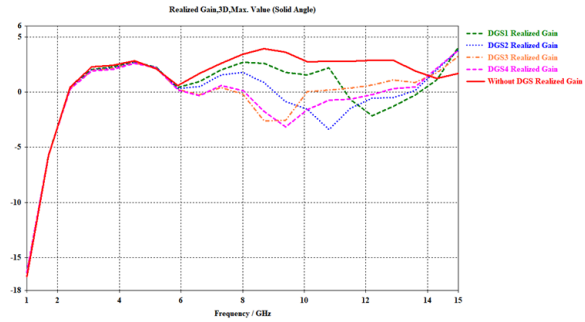

Figure 6. Realized gain of UWB Antenna without DGS and with DGS 1, 2, 3 and 4.

Figures 9, 10, 11 and 12 illustrate the UWB antenna integrated with DGS at three distinct frequencies: 2 GHz, 3.5 GHz, and 6 GHz. These frequencies were specifically chosen for analysis to demonstrate the passband at 3.5 GHz and the rejection bands at frequencies ≤2 GHz and ≥6 GHz. The DGS structure was carefully designed to suppress signals within the rejection bands while ensuring a strong current distribution at 3.5 GHz. Examination of the figures reveals a good current distribution at the designated 3.5 GHz frequency. Conversely, for the rejection bands at 2 GHz and 6 GHz, the current exhibits only relatively stronger presence along the transmission line. This attenuation is attributed to the deliberate suppression of current within these frequency bands by the DGS structure.

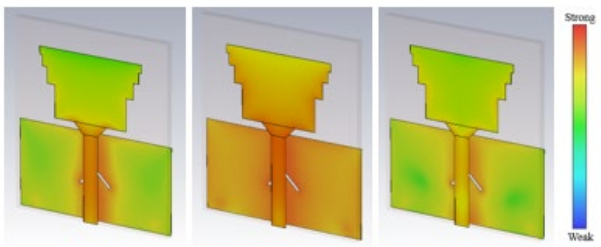

(a) (b) (c)

Figure 9. Surface current of antenna with DGS 1 at (a) 2 GHz (b) 3.5 GHz (c) 6 GHz.

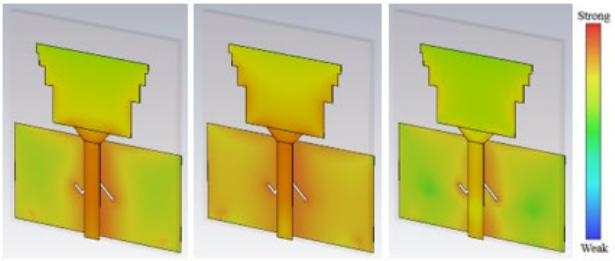

(a) (b) (c)

Figure 10. Surface current of antenna with DGS 2 at (a) 2 GHz (b) 3.5 GHz (c) 6 GHz.

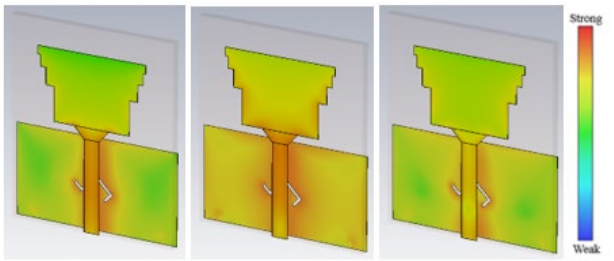

(a) (b) (c)

Figure 11. Surface current of antenna with DGS 3 at (a) 2 GHz (b) 3.5 GHz (c) 6 GHz.

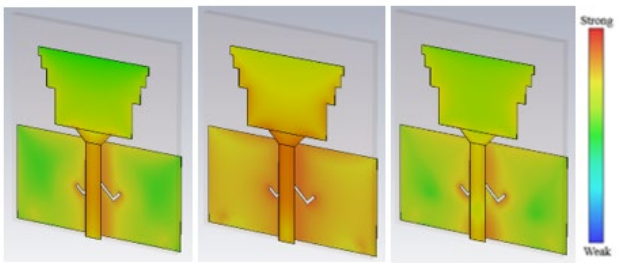

(a) (b) (c)

Figure 12. Surface current of antenna with DGS 4 at (a) 2 GHz (b) 3.5 GHz (c) 6 GHz

4. CONCLUSION

In this study, four distinct DGS designs are investigated for their efficacy in creating a band stop filter focusing on antenna operating frequency on 3.5 GHz for a UWB planar antenna. The performance of each DGS configuration is assessed through simulation, evaluating parameters such as return loss, S-parameters, and radiation characteristics. The results revealed that DGS Design 2 achieved the most desirable outcome, exhibiting a deep stopband centered at 3.5 GHz with minimal impact on the total efficiency, realized gain and surface current. This study provides important insights into the design and optimization of DGS for UWB antenna band stop applications.

REFERENCES

[1] Aiello, G.R. and G.D. Rogerson, *Ultra-wideband wireless systems.* IEEE microwave magazine, 2003. **4**(2): p. 36-47.

[2] Khanh, Q.V., et al., *Wireless communication technologies for IoT in 5G: Vision, applications, and challenges.* Wireless Communications and Mobile Computing, 2022. **2022**: p. 1-12.

[3] Chen, X., *Theory of UWB antenna elements.* Ultra-Wideband Antennas and Propagation for Communications, Radar, and Imaging, 2007: p. 111-145.

[4] Sharma, P., S. Vijay, and M. Shukla, *Ultra-wideband technology: Standards, characteristics, applications.* Helix-The Scientific Explorer| Peer Reviewed Bimonthly International Journal, 2020. **10**(04): p. 59-65.

[5] Arora, S., S. Sharma, and A.K. Rana, *Ultrawide Band Antenna for Wireless Communications: Applications and Challenges.* Internet of Things, 2022: p. 95-106.

[6] Bhat, U.R., K.R. Jha, and G. Singh, *Wide stopband harmonic suppressed low-pass filter with novel DGS.* International Journal of RF and Microwave Computer-Aided Engineering, 2018. **28**(5): p. e21235.

[7] Schantz, H.G. *Three centuries of UWB antenna development*. in *2012 IEEE International Conference on Ultra-Wideband*. 2012. IEEE.

[8] Ashyap, A.Y., et al., *An overview of electromagnetic band-gap integrated wearable antennas.* IEEE Access, 2020. **8**: p. 7641-7658.

[9] Guha, D., S. Biswas, and Y.M. Antar, *Defected ground structure for microstrip antennas.* microstrip and printed antennas: New Trends, Techniques and Applications, 2010: p. 387-434.

[10] Nakmouche, M.F., et al. *Development of H-slotted DGS based dual band antenna using ANN for 5G applications*. in *2021 15th European Conference on Antennas and Propagation (EuCAP)*. 2021. IEEE.

[11] Outerelo, D.A., et al. *Microstrip antenna for 5G broadband communications: Overview of design issues*. in *2015 IEEE international symposium on antennas and propagation & USNC/URSI National Radio Science Meeting*. 2015. IEEE.

[12] Khandelwal, M.K., B.K. Kanaujia, and S. Kumar, *Defected ground structure: fundamentals, analysis, and applications in modern wireless trends.* International Journal of Antennas and Propagation, 2017. **2017**.

[13] Balanis, C.A., *Antenna theory: analysis and design*. 2016: John wiley & sons.

[14] Izuddin, N.Y.N., O. Ayop, and F. Zubir. *A Comparative Study of V-Shaped Slot Effects on DGS and EBG for Wideband Antennas*. in *2023 IEEE International Symposium On Antennas And Propagation (ISAP)*. 2023. IEEE.

[15] Xiao, S., et al., *Mutual coupling suppression in microstrip array using defected ground structure.* IET microwaves, antennas & propagation, 2011. **5**(12): p. 1488-1494.

[16] Salih, R.M. and A.K. Jassim. *Design of Unit Cell for Metamaterials to Enhancement the Characteristic of the Microstrip Antenna*. in *2021 1st Babylon International Conference on Information Technology and Science (BICITS)*. 2021. IEEE.

[17] Kedze, K.E., et al., *Substrate Dielectric Constant Effects on the Performances of a Metasurface-Based Circularly Polarized Microstrip Patch Antenna.* International Journal of Antennas and Propagation, 2022. **2022**.

[18] Ayinala, K.D. and P.K. Sahu. *A Novel DGS-Based Bandstop Filters Integrated Compact Four-Port MIMO Antenna for IEEE 802.11 n/ac WLAN Standards*. in *2021 IEEE MTT-S International Microwave and RF Conference (IMARC)*. 2021. IEEE.